Thermal spin-crossover in the $[M_3Zn_6Cl_6L_{12}]$ (M = Zn, Fe^{II}; L = 5,6-dimethoxy-1,2,3-benzotriazolate) system: structural, electrochemical, Mössbauer, and UV-Vis spectroscopic studies†

Shyam Biswas,[a] Markus Tonigold,[a] Harald Kelm,[b] Hans-Jörg Krüger[b] and Dirk Volkmer*[a,c]

Fusion of pentanuclear Kuratowski-type coordination units leads to homo- and heterononanuclear coordination compounds, two of which are presented, having structural formulae $[Zn_9Cl_6(OMe_2bta)_{12}]\cdot DMF$ (**1**), and $[Fe^{II}_3Zn_6Cl_6(OMe_2bta)_{12}]\cdot DMF$ (**2**), respectively; (OMe_2btaH = 5,6-dimethoxy-1,2,3-benzotriazole; DMF = *N*,*N*′-dimethylformamide). Single crystal X-ray structure analyses reveal the presence of $\{M_3Zn_6L_{12}\}^{6+}$ cores (M = Zn or Fe^{II}; L = 5,6-dimethoxy-1,2,3-benzotriazolate) in which the M^{II} ions are bridged by μ_3-OMe_2bta ligands. In both compounds, the six peripheral Zn ions are tetracoordinated, whereas the remaining three metal ions M are hexacoordinated. The charge of each $\{M_3Zn_6L_{12}\}^{6+}$ moiety is balanced by six chloride anions that are monodentately bound to the peripheral Zn ions. Based on differences in experimental Fe–N-donor bond lengths (deduced from single crystal data of **2** recorded at 223 K), two out of three Fe^{II} ions are found in a high-spin (HS) state, whereas one Fe^{II} ion shows a low-spin (LS) state. The assignment of different energetic ground states of Fe^{II} ions is corroborated by spectroscopic studies: Both solid-state and solution UV-Vis spectra of **2** (at ambient temperature) display absorption bands owing to the presence of both HS and LS Fe^{II} ions. Removal of occluded DMF molecules from the crystal lattices of **1** and **2** in high vacuum leads to fully desolvated powders, termed hereafter **1a** and **2a**, respectively. Mössbauer studies on **2a** show that all three Fe^{II} ions are in HS state at 160 K, and upon cooling to 7 K, the central Fe^{II} ion undergoes a HS→LS transition while the HS states of the other Fe^{II} ions remains unchanged. The cyclic voltammogram of **2** (chloroform solution) exhibits a single reversible oxidation regardless of different Fe^{II} spin states in the nonanuclear core of **2**.

Introduction

The design and synthesis of polynuclear metal complexes with versatile physical and chemical properties are of great current interest in the areas of molecular based electronic, photochemistry and magnetism. The goal is to develop novel materials the properties of which can be controlled by the input of external information. In this context, particular interest has been focused on Fe^{II} spin-crossover (SCO) compounds because they can be considered among the best examples of switchable molecules. In response to external perturbation, distinctive reversible changes occur in the magnetic, structural, dielectric, and optical properties associated with the respective spin state of the SCO materials.[1] Potential applications of SCO materials as molecular switches in information storage and display devices employing these properties have been proposed, described or patented.[2] As a result, interest in the synthesis, structural chemistry and physics of SCO materials has continued to grow.

Six-coordinate Fe^{II} compounds may occur in a paramagnetic high-spin (HS, S = 2) or diamagnetic low-spin (LS, S = 0) state depending on whether the ligand field strength is weak or strong, respectively. For intermediate ligand fields, the energy gap between the excited HS state and the ground LS state may fall in the range of thermal energy. Consequently, a reversible transition between the two states can be induced by variation of temperature, pressure, or light irradiation.[1] Although this energy gap can be tuned in a relatively predictable fashion by varying the strength of the ligand field, this is not the only factor upon which the existence and character of a spin transition depends. This phenomenon is very sensitive to packing effects in the crystal lattice of the compounds, and entities such as lattice solvent molecules or counterions may have a drastic influence on SCO properties of the material.[1d,3m]

The synthesis of new Fe^{II} SCO compounds is of outmost importance for this research area, particularly when the syntheses have to be performed in a controlled manner with the aim of obtaining compounds exhibiting anticipatable SCO behaviours. Unfortunately, an unambiguous predictive method for the rational design of a new Fe^{II} SCO compound is still not available, as pointed

[a]*Ulm University, Institute of Inorganic Chemistry II, Materials and Catalysis, Albert-Einstein-Allee 11, D-89081, Ulm, Germany*

[b]*Technische Universität Kaiserslautern, Fachbereich Chemie, Erwin-Schrödinger Strasse, D-67663, Kaiserslautern, Germany*

[c]*Institute of Physics, Chair of Solid State Science, Augsburg University, Universitätsstrasse 1, D-86135, Augsburg, Germany. E-mail: dirk.volkmer@physik.uni-augsburg.de; Fax: (+)49 (821) 598-5955; Tel: (+)49 (821) 598-3006*

† Electronic supplementary information (ESI) available: XRPD patterns; IR spectra; TG curves; TG-IR spectra; EDX spectrum; optical micrographs; figures of asymmetric units; detailed cyclic voltammogram; tables containing ICP-AES operating parameters, bond lengths and angles, atomic coordinates and equivalent isotropic displacement parameters, and anisotropic displacement parameters. CCDC reference numbers 778555 and 778556. For ESI and crystallographic data in CIF or other electronic format see DOI: 10.1039/c0dt00556h

out by Gütlich *et al.*[1a] "Fine tuning" of the $[Fe^{II}N_6]$ ligand field strength is often required, if the SCO condition is not obtained at first attempt. Experience has led to "rules of thumb" in choosing the successful combination of ligands which will yield the ligand field strength required to induce SCO of the coordinated Fe^{II} ion, and these are generally aromatic heterocyclic N-donors (pyridines, 1,2,4-triazoles, tetrazoles, pyrazoles, imidazoles, thiazoles, thiazolines, isoxazoles, pyrazines, pyridazines), being present either as monodentate ligands or as polydentate chelate ligands, often in combination with monodentate N-bonded NCX^- (X = S, Se) ligands.[1] As far as we are aware, no report on Fe^{II} SCO compounds containing μ_3-bridging 1,2,3-triazolate ligands has appeared up to now. Herein, we present the syntheses and characterization of $[Fe_3Zn_6Cl_6(OMe_2bta)_{12}]\cdot DMF$ (**2**) and its desolvated form (**2a**), the latter representing the first example of a Fe^{II} SCO compound containing the OMe_2bta ligand.

The particular development of compounds **1** and **2** of this report was stimulated by our previous work on Kuratowski-type homo- and heteropentanuclear coordination compounds (Fig. 1) represented by structural formulae $[MZn_4Cl_4(Me_2bta)_6]\cdot$(solvent) (M = Zn, Fe^{II}, Co^{II}, Ni^{II}, or Cu^{II}; Me_2bta = 5,6-dimethyl-1,2,3-benzotriazolate; solvent = DMF or bromobenzene),[4b–c] and the fact that these coordination units can be fused into oligonuclear compounds,[4e] or even into metal–organic frameworks.[4f] Magnetic, structural and UV-Vis spectroscopic investigations on the heteropentanuclear compound $[FeZn_4Cl_4(Me_2bta)_6]$ from the series referred to above, however, indicated the presence of a weak ligand field, thus leading to a HS state of the central hexacoordinated Fe^{II} ion in this particular compound.[4c] In order to tailor a stronger ligand field, we envisaged the ligand OMe_2bta instead of Me_2bta in the syntheses of the compounds presented here, expecting the former ligand to provide more field strength around Fe^{II} ions due to the electron-donating ability of the methoxy substituents of the 1,2,3-benzotriazolate moieties. Though numerous attempts were undertaken to obtain pentanuclear compounds of the formula $[FeZn_4Cl_4(OMe_2bta)_6]$, all synthetic efforts led to compound **2**, which could be formally derived from two lacunary Kuratowsky-type coordination units $[FeZn_3Cl_3L_6]^-$ being fused *via* a shared hexacoordinate Fe ion in the centre of the nonanuclear coordination unit.

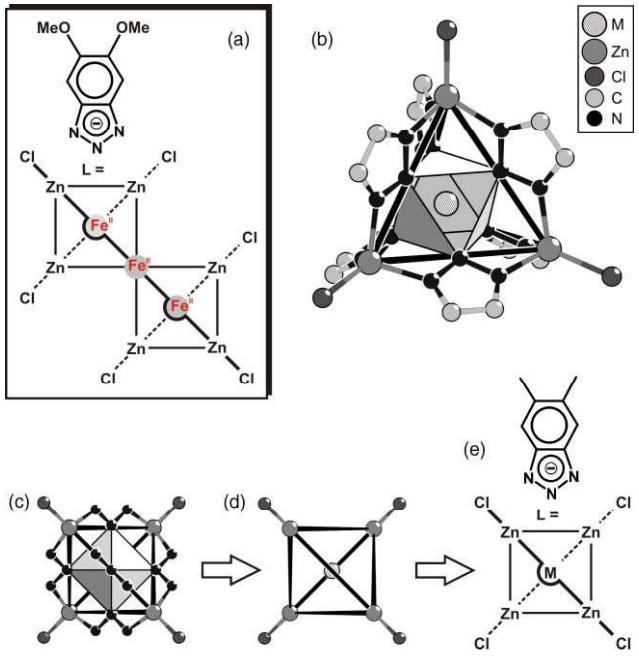

Fig. 1 (a) Skeletal formula representing the connectivity of $[Fe^{II}_3Zn_6Cl_6(L_{12})]$ units (L: 5,6-dimethoxy-1,2,3-benzotriazolate) present in compound **2**. The structure of this compound is formally obtained from fusing two Kuratowsky-type pentanuclear coordination units, a ball-and-stick-model of which is shown in (b). (c–e) Stepwise derivation of a skeletal formula representing the connectivity of $[M^{II}Zn_4X_4(L_6)]$ Kuratowski-type units (X: terminal ligand, L: 1,2,3-triazolate-type ligand) as described in ref. 4b.

Spectroscopic properties of compounds **2** and **2a** were studied in detail in order to investigate the possibility of HS↔LS transitions. Mössbauer measurements show that the central Fe^{II} ion, which bridges the lacunary Kuratowski-type $[FeZn_3Cl_3L_6]^-$ units in **2a** indeed changes its HS state upon cooling. Noteworthingly, the central Fe^{II} ion in a previously reported linear trinuclear Fe^{II} compound, $[Fe_3(Ettrz)_6(H_2O)_6][(CF_3SO_3)_6]$ (Ettrz = 4-ethyl-1,2,4-triazole) showed analogous SCO behaviour.[3d–e]

Compound $[Zn_9Cl_6(OMe_2bta)_{12}]\cdot DMF$ (**1**) represents an isostructural homononanuclear analogue of **2**, which serves as reference sample in the following studies. Afterwards, it was obtained from a directed synthesis. A stoichiometric ratio of suitable metal salts and benzotriazole ligands was used.

In this article, we report on the syntheses, crystal structures, and spectroscopic (especially, electrochemical, Mössbauer and UV-Vis) properties of the above mentioned isostructural homo- and heterononanuclear coordination compounds (**1** and **2**) and their desolvated forms (termed as **1a** and **2a**, respectively).

Experimental

Materials and general methods

The OMe_2btaH ligand was synthesized as described previously.[5] All other starting materials were of reagent grade and used as received from the commercial supplier. Fourier transform infrared (FTIR) spectra were recorded from KBr pellets in the range 4000–400 cm^{-1} on a Bruker IFS FT-IR spectrometer. The following indications are used to characterize absorption bands: very strong (vs), strong (s), medium (m), weak (w), shoulder (sh), and broad (br). UV-Vis diffuse reflectance spectra (DRS) were recorded on an Analytik Jena Specord 50 UV-Vis spectrometer in the range of 300–1100 nm and converted into normal absorption spectra with the Kubelka–Munk function.[6] The lamps change at 320 nm and the mirrors change at 370, 400, 700 and 900 nm. UV-Vis spectra from chloroform solution of compounds **1** and **2** were measured using the same UV-Vis spectrometer. Elemental analyses (C, H, N) were carried out on a Perkin-Elmer 2400 Elemental Analyzer. Thermogravimetric analysis (TGA) was performed with a TGA/SDTA851 Mettler Toledo analyzer in a temperature range of 25–1100 °C in flowing nitrogen gas at a heating rate of 10 °C min^{-1}. TG-IR analysis was carried out using a Netzsch STA 409 simultaneous thermal analyzer coupled with a Bruker IFS 55 Equinox FT-IR spectrometer in a temperature range of 30–1100 °C under N_2 atmosphere with a heating rate of 10 °C min^{-1}. Ambient temperature X-ray powder diffraction (XRPD) patterns were measured using a Philips X'Pert PRO powder diffractometer

operated at 40 kV, 40 mA for Cu target (λ = 1.5406 Å) with a scan speed of 30 s step^{-1} and a step size of 0.008°. The simulated powder patterns were calculated using data from single crystal X-ray diffraction. Energy dispersive X-ray analysis (EDX) was performed on an EDAX (Phönix) X-ray detection system with 30 mm^2 SUTW window. ICP-AES analysis was carried out with a Thermo Scientific iCap 6500 emission spectrometer. Cyclic voltammetry experiments were performed with a computer-controlled VoltaLab 40 PGZ301 potentiostat (Radiometer Analytical, France) in a three-electrode single-compartment cell with a glassy carbon working electrode, a platinum wire counter electrode, and an Ag/AgCl reference electrode. All potentials were internally referenced to the ferrocene/ferrocenium (Fc/Fc^+) couple. Mössbauer spectra were recorded with a conventional spectrometer (Wissel GmbH, Germany) in a constant acceleration mode. The temperature can be maintained between 6 K and 400 K by a closed-cycle cryostat unit (Advanced Research Systems Inc., USA). The sample holder is mounted on the tip of the second stage heat station of the expander unit DE204SF inside a radiation shield and a vacuum shroud. The expander unit is decoupled from the vibrations of the compressor ARS-4HW by a DMX20-41 interface. The temperature is controlled by a Lakeshore 331S unit. The sample was diluted in lactose and placed between aluminium foils in the sample holder. Thus, below 30 K the accuracy of the temperature is within 1 K. The windows of the vacuum shroud are made of mylar foils. The spectra were analyzed by least-square fits using a Lorentzian line shape with the program WinNormus-for-Igor Version 2.0. The isomer shifts are given relative to α-iron at room temperature.

Safety Note! Perchlorate salts and benzotriazolate complexes are potentially explosive, and caution should be exercised when dealing with such materials. However, the small quantities used in this study were not found to present a hazard.

Syntheses

$[Zn_9Cl_6(OMe_2bta)_{12}]\cdot DMF$ (1).

Solvothermal Method. A mixture of anhydrous $ZnCl_2$ (0.05 g, 0.36 mmol) and OMe_2btaH (0.09 g, 0.50 mmol) was dissolved in 4 mL of DMF and the solution was placed in a heating tube (10 mL). The tube was sealed and heated at 120 °C for 20 h, then cooled spontaneously to room temperature. The supernatant was removed and the remaining colorless block-shaped crystals of **1** were washed with DMF (3 × 1 mL) and dried in air to yield 0.06 g (0.02 mmol, 49%). Anal. Calcd for $C_{96}H_{96}Cl_6N_{36}O_{24}Zn_9$: C, 39.47; H, 3.44; N, 17.20. Found: C, 39.26; H, 3.39; N, 17.06%. IR (KBr, cm^{-1}): 3471 (br), 3087 (w), 3004 (w), 2939 (m), 2834 (w), 1729 (w), 1628 (w), 1581 (w), 1497 (vs), 14562 (m), 1441 (m), 1332 (s), 1296 (m), 1223 (vs), 1188 (sh), 1166 (vs), 1013 (s), 888 (s), 832 (s), 798 (sh), 738 (w), 728 (w), 601 (w), 501 (m).

Vapor Diffusion Method. A mixture of anhydrous $ZnCl_2$ (0.05 g, 0.36 mmol) and OMe_2btaH (0.09 g, 0.50 mmol) was placed in a small vial (5 mL) and dissolved in 3 mL of DMF. The vial was then placed in a larger vial (30 mL) containing 6 mL of DMF and 113 µL of 2,6-lutidine. The larger vial was sealed and left undisturbed for 5 days. The resulting colorless block-shaped crystals of **1** were collected by filtration, washed with DMF (3 × 1 mL) and dried in air. The yield was 0.07 g (0.02 mmol, 57%). This material exhibited the same analytical results as the one obtained by the solvothermal method.

$[Fe_3Zn_6Cl_6(OMe_2bta)_{12}]\cdot DMF$ (2).

Solvothermal Method. A mixture of $Fe(ClO_4)_2\cdot 6H_2O$ (0.05 g, 0.20 mmol), anhydrous $ZnCl_2$ (0.05 g, 0.36 mmol) and OMe_2btaH (0.13 g, 0.72 mmol) was dissolved in 4 mL of DMF and the solution was placed in a glass tube (10 mL). The tube was sealed and heated at 120 °C for 20 h, then cooled spontaneously to room temperature. The resulting red block-shaped crystals of **2** were collected by filtration, washed with DMF (3 × 1 mL) and dried in air to yield 0.07 g (0.02 mmol, 38%). Anal. Calcd for $C_{96}H_{96}Cl_6Fe_3N_{36}O_{24}Zn_6$: C, 39.85; H, 3.47; N, 17.36. Found: C, 39.68; H, 3.42; N, 17.19%. IR (KBr, cm^{-1}): 3431 (br), 3088 (w), 3005 (w), 2940 (m), 2834 (w), 1729 (w), 1627 (w), 1676 (m), 1581 (w), 1496 (vs), 1462 (m), 1442 (m), 1331 (s), 1296 (m), 1223 (vs), 1188 (sh), 1166 (vs), 1013 (s), 888 (s), 833 (s), 798 (sh), 737 (w), 728 (w), 601 (w), 501 (m).

Vapor Diffusion Method. A mixture of $Fe(ClO_4)_2\cdot 6H_2O$ (0.05 g, 0.20 mmol), anhydrous $ZnCl_2$ (0.05 g, 0.36 mmol) and OMe_2btaH (0.13 g, 0.72 mmol) was placed in a small vial (5 mL) and dissolved in 3 mL of DMF. The vial was then placed in a larger vial (30 mL) containing 6 mL of DMF and 182 µL of 2,6-lutidine. The larger vial was sealed and left undisturbed for 10 days. The resulting red block-shaped crystals of **2** were collected by filtration, washed with DMF (3 × 1 mL), and dried in air. The yield was 0.08 g (0.03 mmol, 44%). The material obtained by the vapour diffusion method showed the same analytical results as the one obtained by the solvothermal method.

Structure determination

Structures of **1** and **2** were determined from single crystal X-ray data. Since the as-synthesized crystals of each compound "age" rapidly at ambient conditions, they were covered with polybutene oil after being removed from the mother liquor for X-ray diffraction studies. Diffraction measurements of both compounds were performed on a STOE IPDS diffractometer employing monochromated Mo-Kα radiation (λ = 0.71073) at T = 223 K. Initial structures were solved by direct methods and refined by full-matrix least-squares techniques based on F^2 using the SHELXL-97 program.[7] All non-hydrogen atoms were refined anisotropically. CCDC reference numbers 778555 and 778556 for **1** and **2**, respectively. Details of single crystal data collection and refinement of **1** and **2** are summarised in Table 1. All structural plots were drawn using Diamond 3.0 software.[8]

Results and discussion

Syntheses

Compounds **1** and **2** were synthesized applying our previously established strategy[4b] which was used to prepare homo- and heteropentanuclear compounds of the type $[MZn_4Cl_4L_6]$. In these synthetic procedures, a weakly coordinating base such as 2,6-lutidine is introduced into a DMF solution *via* vapor diffusion. The solution contains the metal salt(s) and benzotriazole ligands at the stoichiometric ratio. The auxiliary base (2,6-lutidine) presumably abstracts the acidic –NH protons of benzotriazole ligands that become coordinated to the metal ions. Both compounds **1** and **2** have also been prepared by a solvothermal method employing

Table 1 Single crystal X-ray data and structure refinement parameters for **1** and **2**

Compound	**1**	**2**
Formula	$C_{96}H_{96}Cl_6N_{36}O_{24}Zn_9$	$C_{96}H_{96}Cl_6Fe_3N_{36}O_{24}Zn_6$
Formula mass	2939.12	2910.72
T/K	223(2)	223(2)
λ/Å	0.71073	0.71073
Crystal dimensions/mm	$0.19 \times 0.31 \times 0.42$	$0.08 \times 0.15 \times 0.46$
Crystal system	Monoclinic	Monoclinic
Space group	$P2_1/n$	$P2_1/n$
a/Å	21.848(4)	19.847(4)
b/Å	15.490(3)	15.759(3)
c/Å	22.499(5)	28.428(6)
α (°)	90.00	90.00
β (°)	99.02(3)	110.43(3)
γ (°)	90.00	90.00
V/Å^3	7520(3)	8332(3)
Z	2	2
D_c/g cm^{-3}	1.298	1.160
μ/mm^{-1}	1.581	1.257
$F(000)$	2976	2952
θ Range/°	2.26–25.93	1.69–24.02
Measured reflections	58162	45149
Independent reflections/Rint	14496/0.0691	13026/0.1171
Data/restraints/parameters	14496/0/784	13026/0/774
R_1 ($I > 2\sigma(I)$)[a]	0.0645	0.0901
wR_2 (all data)[b]	0.2319	0.2949
Goodness-of-fit on F^2	1.056	1.059
$\Delta\rho_{max, min}$/e Å^{-3}	1.678, –0.428	2.362, –0.693

[a] $R_1 = \Sigma \| F_o \| - \| F_c \| / \Sigma | F_o |$. [b] $wR_2 = \{\Sigma [w(F_o^2 - F_c^2)^2] / \Sigma [w(F_o^2)^2]\}^{1/2}$.

stoichiometric quantities of appropriate metal salts and benzotriazole ligands dissolved in DMF. The gradual decomposition of DMF under solvothermal condition liberates the base (dimethylamine) in the reaction medium. The base generated *in situ* is essential for the abstraction of the acidic –NH protons from the coordinated benzotriazole ligands. The synthetic procedures leading to **1** and **2** are summarized in Scheme 1.

Compound **1**:

$$9\ ZnCl_2 + 12\ OMe_2btaH + 12\ B \xrightarrow[RT/\triangle]{DMF} [Zn_9Cl_6(OMe_2bta)_{12}] + 12\ BH^{\oplus} + 12\ Cl^{\ominus}$$

Compound **2**:

$$3\ Fe(ClO_4)_2{\cdot}6H_2O + 6\ ZnCl_2 + 12\ OMe_2btaH + 12\ B \xrightarrow[RT/\triangle]{DMF}$$

$$[Fe_3Zn_6Cl_6(OMe_2bta)_{12}] + 12\ BH^{\oplus} + 6\ Cl^{\ominus} + 6\ (ClO_4)^{\ominus} + 18\ H_2O$$

Scheme 1 Chemical equations for the syntheses of **1** and **2**. B is the base 2,6-lutidine for the room temperature (RT) synthesis, or *in situ* generated base dimethylamine for the solvothermal (△) synthesis.

Both compounds are stable in air at ambient conditions. They are soluble in chloroform, 1-methyl-2-pyrrolidone (NMP), *N*,*N*′-dimethylacetamide (DMA), and dimethyl sulfoxide (DMSO).

Characterization

Phase purity of the two metal compounds was confirmed by elemental analysis and X-ray powder diffractometry (XRPD). The experimental XRPD patterns are consistent with the simulated ones as determined from the single crystal X-ray diffraction data (Fig. S1 and S2, ESI†). The experimental XRPD patterns of **1** and **2**, synthesized both *via* solvothermal and vapor diffusion method, are expectedly similar (Fig. S3, ESI†).

The FT-IR spectra of **1** and **2** (Fig. S4 and S5, ESI†) exhibit characteristic strong bands of the coordinated benzotriazolate ligand at *ca.* 1000 cm^{-1} assigned for C–H out-of-plane bending vibrations.[9] Since **1** and **2** are isostructural, their IR spectra are anticipatedly similar. The absorption band at *ca.* 1680 cm^{-1} in the IR spectra of the as-synthesized **1** and **2** is due to the C=O stretching frequency of non-coordinated DMF molecules.[4d] The occluded DMF molecules can be removed from the void regions of the crystal lattices of **1** and **2** if samples are kept for 10 h in vacuum at room temperature. The absence of the strong absorption bands at *ca.* 1680 cm^{-1} in the FT-IR spectra of the fully desolvated samples (**1a** and **2a**) confirms the complete removal of DMF molecules.

In order to examine the thermal stability of the compounds, thermogravimetric analyses (TGA) were performed on the polycrystalline samples of **1** and **2** in nitrogen atmosphere. In the TG traces of the as-synthesized samples of **1** and **2** (Fig. S6 and S7, ESI†), the first weight loss steps (2.15%, **1**; 1.76%, **2**) in the temperature range 80–150 °C is attributed to the loss of one DMF molecule per formula unit (calcd.: 2.42%, **1**; 2.44%, **2**). No further weight loss steps are observed until 400 °C, when the compounds start to decompose. The fully desolvated samples (**1a** and **2a**) show no weight loss until 400 °C (Fig. S6 and S7, ESI†), suggesting complete removal of occluded DMF molecules.

TG-IR analyses were carried out in order to identify the occluded solvent molecules present inside the void regions of **1** and **2**. The existence of volatile DMF molecules, liberated by heating the as-synthesized samples of **1** and **2**, was confirmed by TG-IR analysis (Fig. S8 and S9, ESI†). In the FT-IR spectra of the volatile molecules removed from **1** and **2** at 130 °C, the strong absorption band at *ca.* 1715 cm^{-1} is due to the C=O stretching frequency of gaseous DMF molecules.

An EDX measurement (Fig. S10, ESI†) performed on the single crystals of the hetereononanuclear compound **2** shows that the relative ratio of Fe : Zn is 1 : 2.13, which closely matches with the theoretical ratio (1 : 2.0).

In order to determine the exact amounts of Fe^{II} and Zn^{II} ions present in **2**, ICP-AES analysis was performed on the fully desolvated sample (**2a**) of this compound. The experimental weight percentages of Fe^{II} and Zn^{II} ions are 5.79 and 13.60, respectively. These values match quite closely with the theoretical weight percentages (calcd. for $C_{96}H_{96}Cl_6Fe_3N_{36}O_{24}Zn_6$: Fe = 5.75%, Zn = 13.47%). The emission intensity measurements were made under the conditions summarized in Table S1, ESI†.

Structure description

The structures of the nonanuclear compounds can be deduced from pentanuclear Kuratowski-type coordination units having $\{MZn_4L_6\}^{4+}$ (M = Zn, Fe^{II}, Co^{II}, Ni^{II}, or Cu^{II}; L = 1,2,3-benzotriazolate) cores, which have been previously described by the Volkmer group.[4b,c] In the pentanuclear compounds, six tridentate Me_2bta ligands are coordinated to the central M^{II} ion (Fig. 1). The six triazolate ligands span a Cartesian coordinate system with the Cartesian axes running through the octahedral M^{II} ion at the origin and the N^2 donor atoms of the coordinated ligands. The Me_2bta ligands are twisted around their coordinative

bond to the central M^{II} ion such that the N^2 donor atoms are placed on the edges of an imaginary tetrahedron. At the corners of this tetrahedron are placed four additional Zn^{II} ions which are coordinated to three Me_2bta ligands (*via* their N^1 and N^3 donor atoms) and one chloride anion. Following this, the structures of the nonanuclear compounds described herein can be derived from fusing two tetrahedral lacunary $\{MZn_3Cl_3L_6\}^-$ cores *via* a shared metal ion that is placed in the centre (Fig. 2). In the asymmetric unit of the crystallographic unit cell the common metal(II) ion resides on an inversion center. For both compounds, the edges of the two fused coordination tetrahedra fall in the range of 5.75–6.01 Å. Each of the central metal(II) ions of the tetrahedra lies at a distance of 3.53–3.77 Å from the peripheral ones.

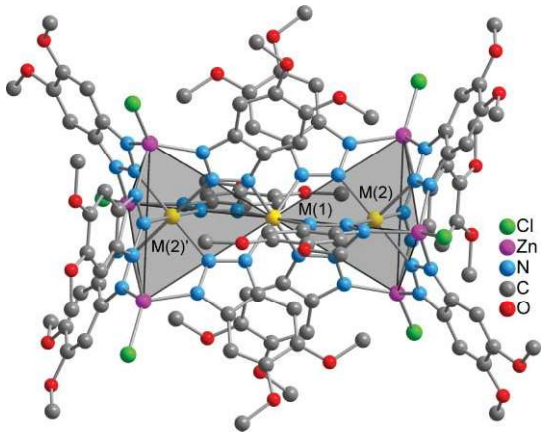

Fig. 2 Ball-and-stick representation of the molecular structures of **1** and **2**. The positions of metal ions are indicated by two inscribed imaginary tetrahedra sharing a common apex (M = Zn, **1**; Fe^{II}, **2**). The symbol (′) represents the symmetry operator (**1**: –x, –y, –z; **2**: 1–x, –y, –z) used to create equivalent metal atoms from atom positions of the crystallographic asymmetric unit.

X-ray crystallographic analyses reveal that both **1** and **2** crystallize in the monoclinic space group $P2_1/n$. The molecular structures of **1** and **2** are shown in Fig. 2. Both of them contain six tetrahedrally coordinated peripheral Zn^{II} ions, and three octahedral ions M (M = Zn, **1**; Fe^{II}, **2**). Each of the peripheral Zn ions is coordinated to three different OMe_2bta ligands (*via* their N^1 and N^3 donor atoms) and one chloride anion. Thus, six chloride anions bound to the peripheral Zn^{II} ions balance the charges of the $\{M_9L_{12}\}^{6+}$ cores present in each compound. The two octahedral M^{II} ions which reside in the center of the imaginary tetrahedrons are coordinated to six different OMe_2bta ligands *via* their N^2 donor atoms. On the other hand, the octahedral M^{II} ion through which the two imaginary tetrahedrons are connected is bound to six different OMe_2bta ligands *via* their N^1 and N^3 donor atoms. Hence, all the three six-coordinated M^{II} ions in both **1** and **2** reside in an octahedral $[M^{II}N_6]$ ligand field. Notably, the $\eta^1{:}\eta^1{:}\eta^1{:}\mu_3$ coordination mode of benzotriazolate ligands observed in the present compounds was previously documented for a wide variety of coordination compounds and coordination polymers containing Zn,[4] Co^{II},[4b–c,4e,10] Ni^{II},[4e,10b,11] Cu^{II},[12] Tl^{I},[13] and M^{III} (M = Fe, Cr, V)[14] ions, including two mixed-valent copper[15] compounds. Moreover, both **1** and **2** are isostructural with five other formerly reported homononanuclear compounds, each of which bearing a $\{M_9L_{12}\}^{6+}$ (M^{II} = Zn,[4d–e] Co,[4e] Ni;[4e,11c] L = 1,2,3-benzotriazolate) core.

Table 2 Selected bond lengths (Å) of **1**

Zn(1)–N(18)	2.139(6)	Zn(3)–N(10)	2.004(5)
Zn(1)–N(12)	2.139(5)	Zn(3)–N(9)	2.005(6)
Zn(1)–N(15)	2.150(6)	Zn(3)–N(3)	2.011(6)
Zn(2)–N(14)	2.157(6)	Zn(4)–N(16)	2.002(5)
Zn(2)–N(11)	2.160(5)	Zn(4)–N(1)	2.006(6)
Zn(2)–N(2)	2.172(6)	Zn(4)–N(4)	2.014(6)
Zn(2)–N(17)	2.177(5)	Zn(5)–N(7)	1.997(6)
Zn(2)–N(5)	2.197(6)	Zn(5)–N(13)	2.004(6)
Zn(2)–N(8)	2.232(6)	Zn(5)–N(6)	2.012(6)

Table 3 Selected bond lengths (Å) of **2**

Fe(1)–N(18)	2.005(8)	Zn(1)–N(1)	2.019(10)
Fe(1)–N(15)	2.020(8)	Zn(1)–N(6)	2.032(9)
Fe(1)–N(12)	2.026(9)	Zn(1)–N(10)	2.040(9)
Fe(2)–N(11)	2.125(9)	Zn(2)–N(13)	1.992(9)
Fe(2)–N(17)	2.143(9)	Zn(2)–N(4)	2.014(10)
Fe(2)–N(14)	2.165(9)	Zn(2)–N(7)	2.061(10)
Fe(2)–N(8)	2.182(9)	Zn(3)–N(3)	1.990(9)
Fe(2)–N(5)	2.201(9)	Zn(3)–N(16)	2.010(9)
Fe(2)–N(2)	2.219(8)	Zn(3)–N(9)	2.018(9)

Selected bond lengths obtained from single crystal X-ray diffraction data of **1** and **2** are summarized in Table 2 and 3, respectively.

The Zn–N distances for the six tetrahedral Zn^{II} ions in **1** fall into the narrow range of 2.00–2.01 Å. However, the six tetrahedrally coordinated Zn ions in **2** exhibit Zn–N distances with slightly larger deviations (1.99–2.06 Å) compared to that of **1**. For the three octahedral M^{II} ions in both **1** and **2**, the M–N distances fall in a wide range of 2.00–2.23 Å. The Zn–N distances for the central and the two adjacent octahedrally coordinated Zn^{II} ions in **1** range from 2.14–2.15 Å and from 2.16–2.23 Å, respectively. For **2**, the Fe–N distances for the central and the adjacent octahedrally coordinated Fe^{II} ions show bond length variations from 2.00–2.03 Å and 2.13–2.22 Å, respectively. Noteworthingly, the central, octahedral M^{II} ions in each compound have smaller M–N distances than the two adjacent octahedrally coordinated M^{II} ions. For **2**, the difference between the average Fe–N distances for the central (Fe(1)) and the adjacent (Fe(2)) ions is 0.16 Å. This significant difference between the Fe–N distances of two crystallographically unique Fe^{II} ions indicates that the Fe^{II} ions are in different spin states, of which the LS state can be tentatively assigned to the central Fe^{II} ion, which rests in a more compressed coordination cage if compared to the other Fe ions (all data refering to the single crystalline state at a temp. of 223 K). Similar values of Fe–N distances with large difference between them ($\Delta r = r_{HS} - r_{LS} \approx 2.20–2.00 \approx 0.20$ Å) have been documented in literature for LS and HS Fe^{II} ions, respectively, in compounds bearing octahedral $[Fe^{II}N_6]$ units.[3] Crystallographic studies on the heteropentanuclear Fe^{II} compound, $[FeZn_4Cl_4(Me_2bta)_6]\cdot 2DMF$ reveal an average Fe–N distance of 2.198(8) Å, indicating the compound to be present in HS state at 298 K.[4c] Noteworthingly, the existence of one LS (central) and two HS Fe^{II} ions has been previously reported by Reedijk *et al.* in the crystal structure of the linear trinuclear Fe^{II} compound, $[Fe_3(Ettrz)_6(H_2O)_6][(CF_3SO_3)_6]$ at 105 K.[3d–e] The different M–N distances for all the three octahedral M^{II} ions in both **1** and **2** suggest that they are in

distorted octahedral [$M^{II}N_6$] environments. The distortion of the octahedral geometry around each M^{II} ion in both compounds is also reflected in the deviation of N–M–N angles (Table S3 and S7, ESI†) from right (90°) and straight angles (180°). The values of Zn–N distances observed in the present compounds fall in the typical range of distances from 1.98–2.22 Å for tetrahedral Zn^{II} and 2.14–2.25 Å for octahedral Zn^{II},[4d–e] as reported previously for structurally similar homononanuclear Zn^{II} triazolate compounds.

Though the coordination compounds **1** and **2** are isostructural, they pack in slightly different ways within the crystal lattices, as displayed in Fig. 3. The occluded DMF molecules in **1** and **2** are highly disordered, thus it was impossible to refine their positions from the electron density distribution obtained from X-ray diffraction data, even with reduction of crystallographic symmetry. The SQUEEZE routine implemented in the program PLATON[16] was used for further analyses of the void regions of both compounds (but no corrections of the scattering intensities were performed). The estimation with the SQUEEZE routine in PLATON using the single crystal data of **2** reveals that the total potentially accessible void volume per unit cell volume is 3428 $Å^3$ which is 41% of the unit cell volume and centered at (0.186, 0.284, 0.160). If calculated using crystallographic atom positions with the same program, slightly smaller values (2360 $Å^3$ and 31%) are obtained for **1** in which the void volume is centered at (0, 0, 0.5). These void volumes (Fig. 3) are occupied by the occluded DMF molecules at ambient conditions, as suggested by TG-IR analysis. Interestingly, the asymmetric units of **1** and **2** (Fig. S13 and 14, ESI†) contain 86 atoms (excluding the hydrogen atoms), and resemble the molecular structures of the pentanuclear compounds shown in Fig. 1, except for the fact that the former lacks one chlorine atom.

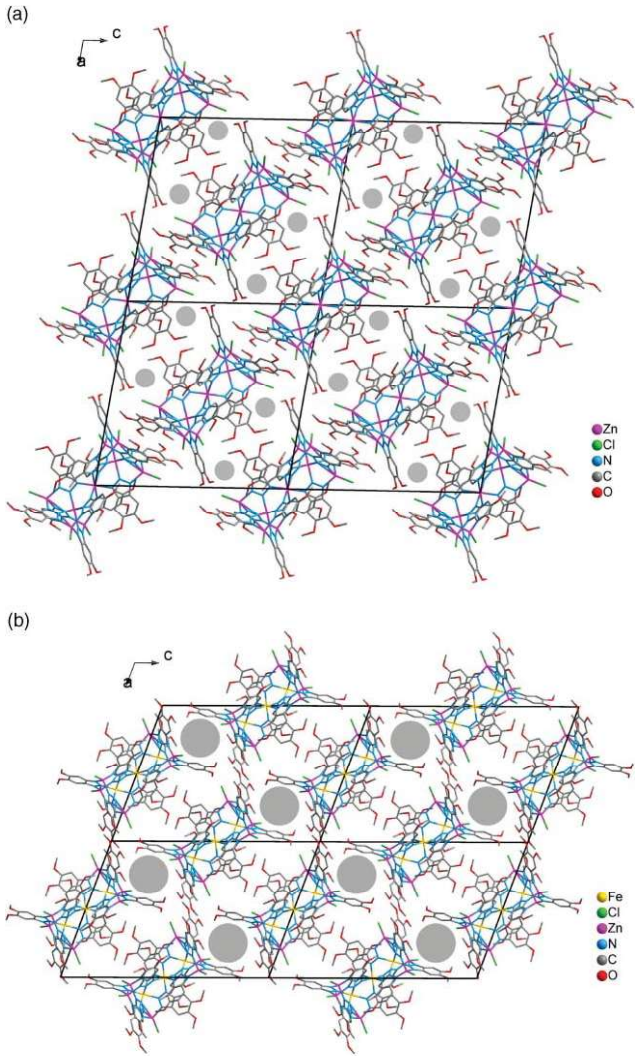

Fig. 3 Wire representations of crystal packing arrangements of (a) **1** and (b) **2**, viewed along the crystallographic *b*-axis. The grey circles represent void regions in the crystal lattices which are occupied by solvate DMF molecules.

UV-Vis spectroscopy

The UV-Vis spectra (Fig. 4a) of **2** in chloroform solution recorded at room temperature, displays one strong absorption band at 390 nm (ε = 45,700 L mol^{-1} cm^{-1}), which can be assigned to a metal-to-ligand charge transfer (MLCT) from the occupied d orbitals of the Fe^{II} ions to the empty π^* orbitals of the OMe_2bta ligands.[17] MLCT bands at analogous positions have been reported for a series of octahedral Fe^{II} compounds with N-donor ligands.[18] In addition, **2** exhibits two weak absorption bands at 850 and 540 nm (respective ε values are 41 and 1150 L mol^{-1} cm^{-1}) owing to the d–d transitions of the octahedrally coordinated HS and LS Fe^{II} ions, respectively.[17] The absorption peak at 540 nm is probably due to transition from $^1A_{1g}$ to $^1T_{2g}$, whereas the weak, broad absorption peak at 850 nm is attributed to transitions from $^5T_{2g}$ to ^5E_g. Absorption bands at similar positions for both HS and LS Fe^{II} ions have been previously observed in the Fe^{II} compound, $[Fe_3(Ettrz)_6(H_2O)_6][(CF_3SO_3)_6]$ at 77 K in solid-state.[3d–e]

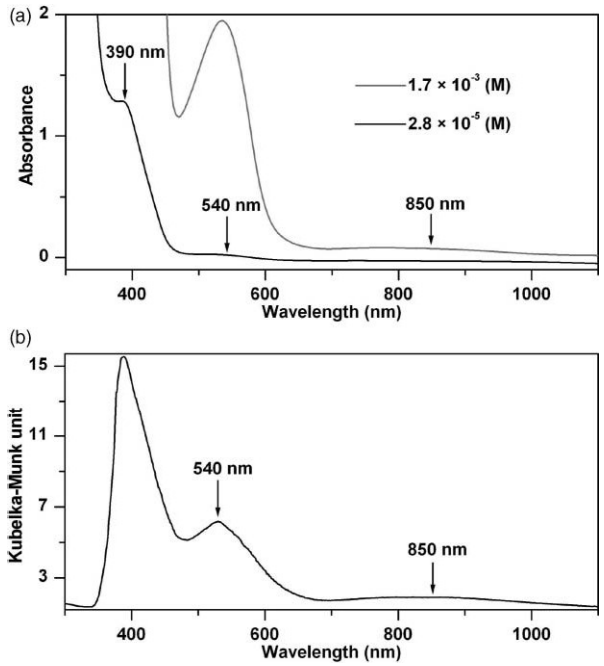

Fig. 4 (a) Room temperature UV-Vis spectra of **2** in $CHCl_3$ solution recorded at two different concentrations (2.8×10^{-5} M, black; 1.7×10^{-3} M, grey). (b) Solid state UV-Vis spectrum of **2** calculated from a diffuse reflection spectrum recorded from a fully desolvated powder sample.

The solid state UV-Vis spectrum (Fig. 4b) of **2** recorded at room temperature exhibits bands similar to those found in the solution UV-Vis spectrum. The similar position of absorption bands in both the solid-state and solution UV-Vis spectra recorded at room temperature provide substantial evidence for the fact that all three Fe^{II} ions retain their octahedral coordination environment in solution.

Electrochemical behaviour

The cyclic voltammogram (CV) of **2** in chloroform solution recorded at room temperature is shown in Fig. 5.

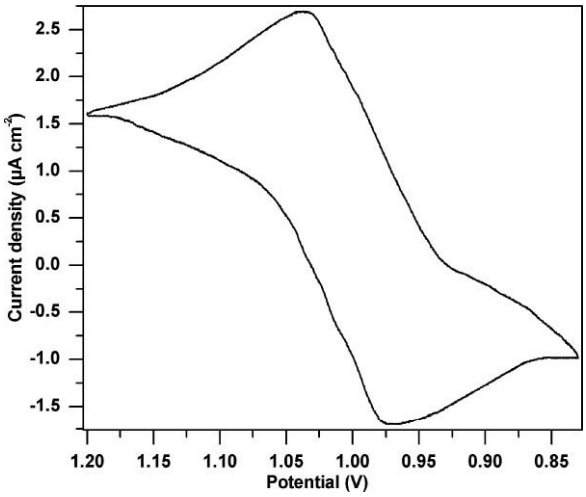

Fig. 5 Room temperature cyclic voltammogram of **2** in $CHCl_3$ with 1.0 (M) [*n*-Bu_4N][PF_6], at a potential scan rate of 0.01 V s^{-1} at a glassy carbon electrode using Ag/Ag^+ as quasi-reference electrode and Fc/Fc^+ as internal reference.

The CV of **2** shows a one-electron transfer attributed to the oxidation of Fe^{II} to Fe^{III} ion. The values of cathodic and anodic peak potentials (E_{pc} and E_{pa}) evaluated from the CV at a potential scan rate of 0.01 V s^{-1} are 1.04 and 0.98 V *vs.* Ag/Ag^+ quasi-reference electrode, respectively. The oxidation process is reversible, since the difference between the cathodic and anodic peak potentials ($\Delta E_p = E_{pc} - E_{pa} = 0.06$ V) remains unchanged on variation of potential sweep rate. It seems likely that only one Fe^{II} ion is oxidized; based on the higher nucleophilicity of the nitrogen donor atoms N^1, this oxidation reaction is tentatively attributed to occur at the central Fe^{II} ion. The estimated value of half-wave potential ($E_{1/2}$) for the Fe^{2+}/Fe^{3+} redox couple of **2** *vs.* Ag/Ag^+ quasi-reference electrode is 1.01 V. Employing Fc/Fc^+ ($E_{1/2} = 0.36$ V) as internal reference, the corresponding $E_{1/2}$ value *vs.* Fc/Fc^+ becomes 0.65 V. Thus, the oxidation of **2** occurs at a significantly higher potential compared to ferrocene (Fig. S15, ESI†).

Mössbauer spectroscopy

Due to the easy loss of solvent molecules from the crystalline material **2**, Mössbauer experiments were carried out with the fully desolvated **2a** at 7 K and at 160 K. The resulting spectra are shown in Fig. 6.

The Mössbauer spectrum at 7 K (Fig. 6a) consists of two doublets with relative intensities of 1 : 2 (34 : 66), which is consistent

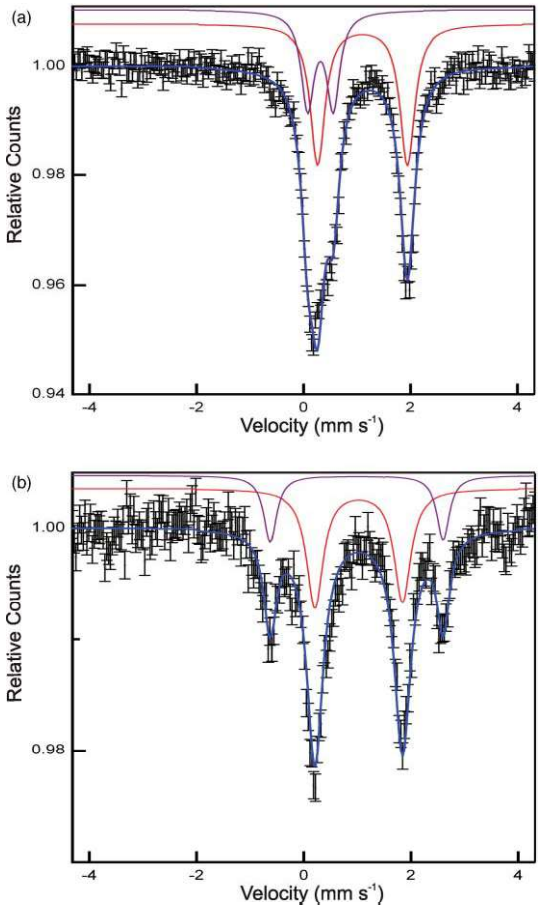

Fig. 6 Mössbauer spectra of **2a** at (a) 7 K and at (b) 160 K. The purple and red subspectra are fitted with the experimental values (black points with error bars).

with the results from the single-crystal structure determination where the peripheral two of the three Fe^{II} ions are related by symmetry due to a crystallographic inversion center and are quite distinct from the third Fe^{II} ion. Based on the isomer shift (δ_{IS}) of 0.43 mm s^{-1} and the quadrupole splitting (ΔE_Q) of 0.48 mm s^{-1}, the less intense signal of the two is attributed to a LS Fe^{II} ion. The second component displays an isomer shift (δ_{IS}) of 1.21 mm s^{-1} and a quadrupole splitting (ΔE_Q) of 1.68 mm s^{-1}. The larger values for the isomer shift and the quadrupole splitting of the second component are clear evidence that the origin of this signal comes from the peripheral HS Fe^{II} ions. A comparison of the results of the Mössbauer spectrum at 7 K with that of the structure determination at 223 K supports the previous assignment of the central iron site to a LS Fe^{II} ion and the peripheral ones to HS Fe^{II} ions. Upon raising the temperature to 160 K, the Mössbauer spectrum (Fig. 6b) shows severe changes. The spectrum is still a superposition of signals arising from two components. The ratio of intensities is, however, now 1 : 3 (25 : 75), which is lower than expected. This might be a consequence of lowering the signal to noise ratio in the Mössbauer spectrum with increasing temperature and/or of different temperature dependencies of the Debye–Waller factors associated with the two contributing iron sites. The larger signal occurs at an isomer shift (δ_{IS}) of 1.13 mm s^{-1} with a quadrupole splitting (ΔE_Q) of 1.63 mm s^{-1}. These parameters are similar to the previous parameters of the larger

signal at 7 K and display the typically observed decrease of δ_{IS} and ΔE_Q values with increasing temperature. The weaker signal, on the other hand, experiences a drastic change. Thus, the new values for δ_{IS} of 1.10 mm s^{-1} and for ΔE_Q of 3.22 mm s^{-1} arising from the central Fe^{II} ion can only be rationalized as the result of a spin crossover during which the central Fe^{II} adopts a HS state at 160 K. The conclusion of a spin crossover process below 160 K is also corroborated by the observation that the powder **2a** changes its color from brownish-yellow to red upon cooling to liquid nitrogen temperatures. The spin state of the central Fe^{II} ion in this powder contrasts with that of the crystalline material. Due to the presence of additional solvent molecules in the crystal lattice, the LS state of the central Fe^{II} ion is stabilized and is still observable at 223 K. The decisive dependence of spin crossover properties on crystal solvent molecules or type of counteranions has already been noted in many other examples.[1d,3m]

Conclusions

We have demonstrated the successful design, synthesis and characterization of the first heterononanuclear Fe^{II} SCO compound, $[Fe_3Zn_6Cl_6(OMe_2bta)_{12}]$ (**2a**) based on a 1,2,3-triazolate ligand. The syntheses, structures and spectroscopic properties of its solvated form (**2**) and homonuclear analogues (**1** and **1a**) are also described. Mössbauer spectroscopic investigations on **2a** reveal a HS→LS transition for only the central Fe(1) ion upon cooling, while the HS states of the two adjacent octahedrally coordinated Fe(2) ions remain unchanged upon variation of temperature. This unique SCO behaviour is rare, and has been previously reported only for a single trinuclear Fe^{II} compound.[3d–e] The different SCO behaviour of the Fe ions in compound **2** can be rationalized in terms of different strengths of the local ligand-fields exerted by each set of N-donor atoms comprising the ligand cage of the Fe centres. Whereas the central Fe(1) ion is coordinated exclusively *via* the more nucleophilic N^1 donor atoms of the benzotriazolate ligands, the coordination environment of the two adjacent Fe(2) ions is formed exclusively by a set of six N^2 donor atoms stemming from the coordinated benzotriazolate ligands. The lower nucleophilicity of the N^2 triazolate donor atoms thus finds its expression in the fact that these Fe(2) centres retain their HS state under all experimental conditions.

Comparative Mössbauer studies on solvated **2** (which does not display SCO behaviour), and desolvated (**2a**) materials suggest that the present Fe^{II} SCO system is very sensitive to the presence of lattice solvent molecules, which is a well-established phenomenon shown by many other SCO systems.[1d,3m] Electrochemical investigations on **2** show a single reversible oxidation, occuring at a potential significantly higher than that of ferrocene. Both, X-ray diffraction studies (223 K) and UV-Vis analyses (298 K) of **2** indicate the presence of both HS and LS Fe^{II} ions at the respective measurement temperatures. Unfortunately, the complicated time-dependent release of solvent DMF molecules results in "aging" of the crystals of **2**, preventing us from performing any further time- and temperature-dependent studies to correlate the magnetic and SCO behaviour of **2** and **2a** at various conditions. Nevertheless, our previous experience[4b–c] on 1,2,3-triazole-based heteropentanuclear compounds indicate that the present SCO system (**2a**) might represent one member of a family of compounds having composition $[M_3Zn_6X_6L_{12}]$, which can be prepared by the variation of 3d transition metal (M^{II} = Co, Ni, or Cu) ions, 1,2,3-triazolate ligands or monodentately coordinated halogenides (X = Cl, Br, or I). Notably, the heterononanuclear Co^{II} compound isostructural with **2** might show interesting SCO behaviour, comparable with **2a**, since SCO in Co^{II} compounds is well-documented, although less commonly observed than for Fe^{II} compounds.[19] Investigations in these directions are in progress in our laboratories and will be reported in due course.

Acknowledgements

The authors are grateful to financial support from the German Research Foundation (DFG Priority Program 1362 "Porous Metal–Organic Frameworks", VO 829/5-1). M.T. is grateful to the Landesgraduiertenförderung Baden-Württemberg for financial support.

References

1 (*a*) P. Gütlich, Y. Garcia and H. A. Goodwin, *Chem. Soc. Rev.*, 2000, **29**, 419; (*b*) J. A. Real, A. B. Gaspar, V. Niel and M. C. Muñoz, *Coord. Chem. Rev.*, 2003, **236**, 121; (*c*) *Spin Crossover in Transition Metal Compounds I–III, Topics in Current Chemistry*, ed. P. Gütlich and H. A. Goodwin, Springer, Heidelberg, 2004, vol. 233–235; (*d*) J. A. Real, A. B. Gaspar and M. C. Muñoz, *Dalton Trans.*, 2005, 2062.

2 (*a*) O. Kahn, C. Jay, J. Kröber, R. Claude and F. Grolière, *Eur. Pat.*, 0666561, 1995; (*b*) A. Bousseksou, C. Vieu, J.-F. Létard, P. Demont, J.-P. Tuchagues, L. Malaquin, J. Menegotto and L. Salmon, *Int. Pat.*, 019695, 2003; (*c*) J.-F. Létard, P. Guionneau and L. Goux-Capes, *Top. Curr. Chem.*, 2004, **235**, 221; (*d*) J.-F. Létard, O. Nguyen and N. Daro, *Fr. Pat.*, 0512476, 2005.

3 (*a*) E. König and K. J. Watson, *Chem. Phys. Lett.*, 1970, **6**, 457; (*b*) B. A. Katz and C. E. Strouse, *J. Am. Chem. Soc.*, 1979, **101**, 6214; (*c*) M. Mikami, M. Konno and Y. Saito, *Acta Crystallogr., Sect. B: Struct. Crystallogr. Cryst. Chem.*, 1980, **36**, 275; (*d*) G. Vos, R. A. le Fêbre, R. A. G. de Graaff, J. G. Haasnoot and J. Reedijk, *J. Am. Chem. Soc.*, 1983, **105**, 1682; (*e*) G. Vos, R. A. G. de Graaff, J. G. Haasnoot, A. M. Van Der Kraan, P. de Vaal and J. Reedijk, *Inorg. Chem.*, 1984, **23**, 2905; (*f*) L. Weil, G. Kiel, C. P. Köhler, H. Spiering and P. Gütlich, *Inorg. Chem.*, 1986, **25**, 1565; (*g*) L. Wiehl, *Acta Crystallogr., Sect. B: Struct. Sci.*, 1993, **49**, 289; (*h*) M. Thomann, O. Kahn, J. Guilhem and F. Varret, *Inorg. Chem.*, 1994, **33**, 6029; (*i*) J. Jung, F. Bruchhaüser, R. Feile, H. Spiering and P. Gütlich, *Z. Phys. B: Condens. Matter*, 1996, **100**, 517; (*j*) J. J. A. Kolnaar, G. van Dijk, H. Kooijman, A. L. Spek, V. G. Ksenofontov, P. Gütlich, J. G. Haasnoot and J. Reedijk, *Inorg. Chem.*, 1997, **36**, 2433; (*k*) J. J. A. Kolnaar, M. I. de Heer, H. Kooijman, A. L. Spek, G. Schmitt, V. Ksenofontov, P. Gütlich, J. G. Haasnoot and J. Reedijk, *Eur. J. Inorg. Chem.*, 1999, 881; (*l*) Y. Garcia, P. Guionneau, G. Bravic, D. Chasseau, J. A. K. Howard, O. Kahn, V. Ksenofontov, S. Reiman and P. Gütlich, *Eur. J. Inorg. Chem.*, 2000, 1531; (*m*) P. Gütlich and H. A. Goodwin, *Top. Curr. Chem.*, 2004, **233**, 1; (*n*) P. Guionneau, M. Marchivie, G. Bravic, J.-F. Létard and D. Chasseau, *Top. Curr. Chem.*, 2004, **234**, 97; (*o*) J. Kusz, P. Gütlich and H. Spiering, *Top. Curr. Chem.*, 2004, **234**, 129; (*p*) K. Nakano, N. Suemura, S. Kawata, A. Fuyuhiro, T. Yagi, S. Nasu, S. Morimoto and S. Kaizaki, *Dalton Trans.*, 2004, 982; (*q*) B. A. Leita, B. Moubaraki, K. S. Murray, J. P. Smith and J. D. Cashion, *Chem. Commun.*, 2004, 156; (*r*) K. Nakano, S. Kawata, K. Yoneda, A. Fuyuhoro, T. Yagi, S. Nasu, S. Morimoto and S. Kaizaki, *Chem. Commun.*, 2004, 2892; (*s*) M. H. Klingele, B. Moubaraki, J. D. Cashion, K. S. Murray and S. Brooker, *Chem. Commun.*, 2005, 987; (*t*) K. Yoneda, K. Adachi, S. Hayami, Y. Maeda, M. Katada, A. Fuyuhiro, S. Kawata and S. Kaizaki, *Chem. Commun.*, 2006, 45; (*u*) J. A. Kitchen, A. Noble, C. D. Brandt, B. Moubaraki, K. S. Murray and S. Brooker, *Inorg. Chem.*, 2008, **47**, 9450.

4 (*a*) Y.-Y. Qin, J. Zhang, Z.-J. Li, L. Zhang, X.-Y. Cao and Y.-G. Yao, *Chem. Commun.*, 2008, 2532; (*b*) S. Biswas, M. Tonigold and D. Volkmer, *Z. Anorg. Allg. Chem.*, 2008, **634**, 2532; (*c*) S. Biswas, M. Tonigold, M. Speldrich, P. Kögerler, M. Weil and D. Volkmer, *Inorg. Chem.*, 2010, **49**, 7424; (*d*) C. Gkioni, V. Psycharis and C. P.

Raptopoulou, *Polyhedron*, 2009, **28**, 3425; (*e*) S. Biswas, M. Tonigold, M. Speldrich, P. Kögerler and D. Volkmer, *Eur. J. Inorg. Chem.*, 2009, 3094; (*f*) S. Biswas, M. Grzywa, H. P. Nayek, S. Dehnen, S. Senkovska, S. Kaskel and D. Volkmer, *Dalton Trans.*, 2009, 6487; (*g*) X. L. Wang, C. Qin, S.-X. Wu, K.-Z. Shao, Y. Q. Lan, S. Wang, D. S. Zhu, Z.-M. Su and E.-B. Wang, *Angew. Chem., Int. Ed.*, 2009, **48**, 5291.

5 A. Boido, R. Budries, C. C. Boido, P. Ioan, E. Terranova, A. Chiarini and F. Sparatore, *Chem. Biodiversity*, 2005, **2**, 1290.

6 W. W. Wendlandt and H. G. Hecht, *Reflectance Spectroscopy*, Interscience Publishers/JohnWiley & Sons, New York, 1966.

7 G. M. Sheldrick, *SHELXL-97, Program for the Refinement of Crystal Structures*, University of Göttingen, Germany, 1997.

8 K. Brandenburg and H. Putz, *DIAMOND (Version 3.0), Crystal and Molecular Structure Visualization*, Crystal Impact GbR, Bonn, Germany.

9 J. Rubim, I. G. R. Gutz, O. Sala and W. J. Orville-Thomas, *J. Mol. Struct.*, 1983, **100**, 571.

10 (*a*) X.-M. Zhang, Z.-M. Hao, W.-X. Zhang and X.-M. Chen, *Angew. Chem., Int. Ed.*, 2007, **46**, 3456; (*b*) Y.-L. Bai, J. Tao, R. B. Huang and L. S. Zheng, *Angew. Chem., Int. Ed.*, 2008, **47**, 5344.

11 (*a*) E. G. Bakalbassis, E. Diamontopoulou, S. P. Perlepes, C. P. Raptopoulou, V. Tangoulis, A. Terzis and T. F. Zafiropoulos, *J. Chem. Soc., Chem. Commun.*, 1995, 1347; (*b*) V. Tangoulis, C. P. Raptopoulou, A. Terzis, E. G. Bakalbassis, E. Diamontopoulou and S. P. Perlepes, *Inorg. Chem.*, 1998, **37**, 3142; (*c*) V. Tangoulis, C. P. Raptopoulou, A. Terzis, E. G. Bakalbassis, E. Diamontopoulou and S. P. Perlepes, *Mol. Cryst. Liq. Cryst.*, 1999, **335**, 463.

12 (*a*) J. H. Marshall, *Inorg. Chem.*, 1978, **17**, 3711; (*b*) J. Handley, D. Collison, C. D. Garner, M. Helliwell, R. Docherty, J. R. Lawson and P. A. Tasker, *Angew. Chem., Int. Ed.*, 1993, **32**, 1036; (*c*) M. Murrie, D. Collison, C. D. Garner, M. Helliwell, P. A. Tasker and S. S. Turner, *Polyhedron*, 1998, **17**, 3031; (*d*) W. Jinling, Y. Ming, Y. Yun, Z. Shuming and M. Fangming, *Chin. Sci. Bull.*, 2002, **47**, 890.

13 J. Reedijk, G. Roelofsen, A. R. Siedle and A. L. Spek, *Inorg. Chem.*, 1979, **18**, 1947.

14 (*a*) L. F. Jones, E. K. Brechin, D. Collison, A. Harrison, S. J. Teat and W. Wernsdorfer, *Chem. Commun.*, 2002, 2974; (*b*) D. M. Low, L. F. Jones, A. Bell, E. K. Brechin, T. Mallah, E. Rivière, S. J. Teat and E. J. L. McInnes, *Angew. Chem., Int. Ed.*, 2003, **42**, 3781; (*c*) L. F. Jones, E. K. Brechin, D. Collison, J. Raftery and S. J. Teat, *Inorg. Chem.*, 2003, **42**, 6971; (*d*) L. F. Jones, G. Rajaraman, J. Brockman, M. Murugesu, J. Raftery, S. J. Teat, W. Wernsdorfer, G. Christou, E. K. Brechin and D. Collison, *Chem.–Eur. J.*, 2004, **10**, 5180; (*e*) J. Tabernor, L. F. Jones, S. L. Heath, C. Muryn, G. Aromí, J. Ribas, E. K. Brechin and D. Collison, *Dalton Trans.*, 2004, 975; (*f*) L. F. Jones, J. Raftery, S. J. Teat, D. Collison and E. K. Brechin, *Polyhedron*, 2005, **24**, 2443; (*g*) D. Collison, E. J. L. McInnes and E. K. Brechin, *Eur. J. Inorg. Chem.*, 2006, 2725; (*h*) R. H. Laye, Q. Wei, P. V. Mason, M. Shanmugam, S. J. Teat, E. K. Brechin, D. Collison and E. J. L. McInnes, *J. Am. Chem. Soc.*, 2006, **128**, 9020; (*i*) R. Shaw, R. H. Laye, L. F. Jones, D. M. Low, C. Talbot-Eeckelaers, Q. Wei, C. J. Milios, S. Teat, M. Helliwell, J. Raftery, M. Evangelisti, M. Affronte, D. Collison, E. K. Brechin and E. J. L. McInnes, *Inorg. Chem.*, 2007, **46**, 4968.

15 (*a*) V. L. Himes, A. D. Mighell and A. R. Siedle, *J. Am. Chem. Soc.*, 1981, **103**, 211; (*b*) G. F. Kokoszka, J. Baranowski, C. Goldstein, J. Orsini, A. D. Mighell, V. L. Himes and A. R. Siedle, *J. Am. Chem. Soc.*, 1983, **105**, 5627; (*c*) Y.-X. Yuan, P.-J. Wei, W. Qin, Y. Zhang, J.-L. Yao and R.-A. Gu, *Eur. J. Inorg. Chem.*, 2007, 4980.

16 A. L. Spek, *J. Appl. Crystallogr.*, 2003, **36**, 7.

17 (*a*) C. J. Ballhausen, *Introduction to Ligand-Field Theory*, McGraw-Hill, New York, 1962; (*b*) B. N. Figgis, *Introduction to Ligand Fields*, Interscience, New York, 1966; (*c*) A. B. P. Lever, *Inorganic Electronic Spectroscopy*, Elsevier Publishing Company, Amsterdam, 1968, ch. 9, pp. 299-305.

18 H. Toftlund, *Coord. Chem. Rev.*, 1989, **94**, 67.

19 H. A. Goodwin, *Top. Curr. Chem.*, 2004, **234**, 23.